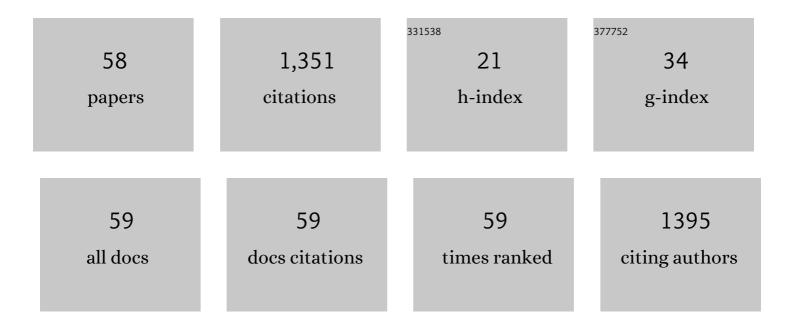
Martine D Buatier

List of Publications by Year in descending order

Source: https://exaly.com/author-pdf/9030807/publications.pdf Version: 2024-02-01



#	Article	IF	CITATIONS
1	Formation of todorokite from vernadite in Ni-rich hemipelagic sediments. Geochimica Et Cosmochimica Acta, 2007, 71, 5698-5716.	1.6	145
2	Deformation and recrystallization mechanisms in naturally deformed omphacites from the Sesia-Lanzo zone; geophysical consequences. Tectonophysics, 1991, 195, 11-27.	0.9	76
3	Smectite-Illite Transition in Barbados Accretionary Wedge Sediments: TEM and AEM Evidence for Dissolution/Crystallization at Low Temperature. Clays and Clay Minerals, 1992, 40, 65-80.	0.6	68
4	Microtectonic and geochemical characterization of thrusting in a foreland basin: Example of the South-Pyrenean orogenic wedge (Spain). Journal of Structural Geology, 2011, 33, 1359-1377.	1.0	54
5	Mechanisms of Mg-phyllosilicate formation in a hydrothermal system at a sedimented ridge (Middle) Tj ETQq1 1	0.784314 1.2	rgBT /Overlo
6	Syntectonic fluid-flow along thrust faults: Example of the South-Pyrenean fold-and-thrust belt. Marine and Petroleum Geology, 2014, 49, 84-98.	1.5	50
7	Fe-Smectite-Glauconite Transition in Hydrothermal Green Clays from the Galapagos Spreading Center. Clays and Clay Minerals, 1989, 37, 532-541.	0.6	46
8	Land use change, soil erosion and alluvial dynamic in the lower Doubs Valley over the 1st millenium AD (Neublans, Jura, France). Journal of Archaeological Science, 2003, 30, 1283-1299.	1.2	42
9	Origin and behavior of clay minerals in the Bogd fault gouge, Mongolia. Journal of Structural Geology, 2012, 34, 77-90.	1.0	40
10	Characterization of metalliferous sediment from a low-temperature hydrothermal environment on the Eastern Flank of the East Pacific Rise. Marine Geology, 2008, 250, 128-141.	0.9	38
11	Characterization and origin of Fe ³⁺ -montmorillonite in deep-water calcareous sediments (Pacific Ocean, Costa Rica margin). Clays and Clay Minerals, 2005, 53, 452-465.	0.6	37
12	TEM-EDX investigation on Zn- and Pb-contaminated soils. Applied Geochemistry, 2001, 16, 1165-1177.	1.4	35
13	Formation of chlorite during thrust fault reactivation. Record of fluid origin and P–T conditions in the Monte Perdido thrust fault (southern Pyrenees). Contributions To Mineralogy and Petrology, 2012, 163, 1083-1102.	1.2	33
14	Clay Diagenesis in the Sandstone Reservoir of the Ellon Field (Alwyn, North Sea). Clays and Clay Minerals, 1999, 47, 269-285.	0.6	32
15	Effect of Pb-rich and Fe-rich entities during alteration of a partially vitrified metallurgical waste. Journal of Hazardous Materials, 2007, 149, 418-431.	6.5	30
16	Conditions and mechanism for the formation of iron-rich Montmorillonite in deep sea sediments (Costa Rica margin): Coupling high resolution mineralogical characterization and geochemical modeling. Geochimica Et Cosmochimica Acta, 2011, 75, 1397-1410.	1.6	28
17	Temperature micro-mapping in oscillatory-zoned chlorite: Application to study of a green-schist facies fault zone in the Pyrenean Axial Zone (Spain). American Mineralogist, 2015, 100, 2468-2483.	0.9	26
18	Fluid–sediment interactions related to hydrothermal circulation in the Eastern Flank of the Juan de Fuca Ridge. Chemical Geology, 2001, 175, 343-360.	1.4	25

MARTINE D BUATIER

#	Article	IF	CITATIONS
19	Mineralogical characterization and genesis of hydrothermal Mn oxides from the flank of the Juan the Fuca Ridge. American Mineralogist, 2004, 89, 1807-1815.	0.9	24
20	Influence of fault rock foliation on fault zone permeability: The case of deeply buried arkosic sandstones (Grès d'Annot, southeastern France). AAPG Bulletin, 2013, 97, 1521-1543.	0.7	23
21	Iron in Hydrothermal Clays from the Galapagos Spreading Centre Mounds: Consequences for the Clay Transition Mechanism. Clay Minerals, 1993, 28, 641-655.	0.2	22
22	Dickite related to fluid-sediment interaction and deformation in Pyrenean thrust-fault zones. European Journal of Mineralogy, 1997, 9, 875-888.	0.4	22
23	Zinc-rich clays in supergene non-sulfide zinc deposits. Mineralium Deposita, 2016, 51, 467-490.	1.7	21
24	CLAY RESOURCES AND TECHNICAL CHOICES FOR NEOLITHIC POTTERY (CHALAIN, JURA, FRANCE): CHEMICAL, MINERALOGICAL AND GRAIN-SIZE ANALYSES*. Archaeometry, 2007, 49, 23-52.	0.6	19
25	Syntectonic fluid flow and deformation mechanisms within the frontal thrust of a foreland fold-and-thrust belt: Example from the Internal Jura, Eastern France. Tectonophysics, 2020, 778, 228178.	0.9	19
26	Formation of phyllosilicates in a fault zone affecting deeply buried arkosic sandstones: their influence on petrophysic properties (Annot sandstones, French external Alps). Swiss Journal of Geosciences, 2012, 105, 299-312.	0.5	17
27	Quantification of mass transfers and mineralogical transformations in a thrust fault (Monte Perdido) Tj ETQq1 1	0.784314 1.5	4 rgBT /Overlo
28	Occurrence of nacrite in the Lodève Permian basin (France). European Journal of Mineralogy, 1996, 8, 847-852.	0.4	17
29	Textural-chemical changes and deformation conditions registered by phyllosilicates in a fault zone (Pic de Port Vieux thrust, Pyrenees). Applied Clay Science, 2017, 144, 88-103.	2.6	16
30	Fluid migration during Eocene thrust emplacement in the south Pyrenean foreland basin (Spain): an integrated structural, mineralogical and geochemical approach. Geological Society Special Publication, 1998, 134, 163-188.	0.8	14
31	Li and Li isotopic composition of hydrothermally altered sediments at Middle Valley, Juan De Fuca. Chemical Geology, 2004, 211, 363-373.	1.4	14
32	Phyllosilicates formation in faults rocks: Implications for dormant faultâ€sealing potential and fault strength in the upper crust. Geophysical Research Letters, 2013, 40, 4272-4278.	1.5	14
33	40Ar/39Ar muscovite dating of thrust activity: a case study from the Axial Zone of the Pyrenees. Tectonophysics, 2018, 745, 412-429.	0.9	14
34	Expedition 385 methods. Proceedings of the International Ocean Discovery Program, 0, , .	0.0	14
35	Microtextural investigation (SEM and TEM study) of phyllosilicates in a major thrust fault zone (Monte Perdido, southern Pyrenees): impact on fault reactivation. Swiss Journal of Geosciences, 2012, 105, 313-324.	0.5	13
36	Earliest salt working in the world: From excavation to microscopy at the prehistoric sites of Ţolici and Lunca (Romania). Journal of Archaeological Science, 2018, 89, 46-55.	1.2	13

MARTINE D BUATIER

#	Article	IF	CITATIONS
37	Site U1545. Proceedings of the International Ocean Discovery Program, 0, , .	0.0	13
38	Clays and zeolite authigenesis in sediments from the flank of the Juan de Fuca Ridge. Clay Minerals, 2002, 37, 143-155.	0.2	12
39	Nature and origin of natural Zn clay minerals from the Bou Arhous Zn ore deposit: Evidence from electron microscopy (SEM-TEM) and stable isotope compositions (H and O). Applied Clay Science, 2016, 132-133, 377-390.	2.6	12
40	Impact of ancient iron smelting wastes on current soils: Legacy contamination, environmental availability and fractionation of metals. Science of the Total Environment, 2021, 776, 145929.	3.9	12
41	The problem of differentiation of glauconite and celadonite. Chemical Geology, 1990, 84, 264-266.	1.4	11
42	Weakening processes in thrust faults: insights from the <scp>M</scp> onte <scp>P</scp> erdido thrust fault (southern <scp>P</scp> yrenees, <scp>S</scp> pain). Geofluids, 2013, 13, 56-65.	0.3	11
43	Site U1546. Proceedings of the International Ocean Discovery Program, 0, , .	0.0	11
44	Evidence of multi-stage faulting by clay mineral analysis: Example in a normal fault zone affecting arkosic sandstones (Annot sandstones). Journal of Structural Geology, 2015, 75, 101-117.	1.0	10
45	Expedition 385 summary. Proceedings of the International Ocean Discovery Program, 0, , .	0.0	10
46	87Sr/86Sr and 18O/16O ratios of clays from a hydrothermal area near the Galapagos rift as records of origin, crystallization temperature and fluid composition. Marine Geology, 2011, 288, 32-42.	0.9	9
47	Fluid–rock interactions related to metamorphic reducing fluid flow in meta-sediments: example of the Pic-de-Port-Vieux thrust (Pyrenees, Spain). Contributions To Mineralogy and Petrology, 2017, 172, 1.	1.2	9
48	Sites U1547 and U1548. Proceedings of the International Ocean Discovery Program, 0, , .	0.0	9
49	Nacrite in the Lodève Permian Basin: a TEM and fluid-inclusion study. European Journal of Mineralogy, 2000, 12, 329-340.	0.4	9
50	Characterization and origin of low-T willemite (Zn2SiO4) mineralization: the case of the Bou Arhous deposit (High Atlas, Morocco). Mineralium Deposita, 2017, 52, 1085-1102.	1.7	7
51	Sedimentary fluids/fault interaction during syn-rift burial of the LodÃ`ve Permian Basin (Hérault,) Tj ETQq1 1 0 Geology, 2017, 88, 303-328.	.784314 r 1.5	gBT /Overlock 7
52	Site U1549. Proceedings of the International Ocean Discovery Program, 0, , .	0.0	7
53	Site U1550. Proceedings of the International Ocean Discovery Program, 0, , .	0.0	6
54	Nd–Sr isotope and REY geochemistry of metalliferous sediments in a low-temperature off-axis hydrothermal environment (Costa Rica margin). Marine Geology, 2012, 315-318, 132-142.	0.9	5

#	Article	IF	CITATIONS
55	Difference in petrophysical properties between foliated and dilatant fault rocks in deeply buried clastics: The case of the GrA¨s d'Annot Formation, <scp>SW</scp> French Alps. Terra Nova, 2014, 26, 298-306.	0.9	5
56	Site U1552. Proceedings of the International Ocean Discovery Program, 0, , .	0.0	4
57	Site U1551. Proceedings of the International Ocean Discovery Program, 0, , .	0.0	3
58	Circulation hydrothermale dans le flanc est de la ride de Juan de Fuca. Résultats du Leg ODP 168. Comptes Rendus De L'Académie Des Sciences Earth & Planetary Sciences Série II, Sciences De La Terre Et Des PlazÃriano - 1008, 220, 201, 201	0.2	0

Des PlanÃ[°]tes =, 1998, 326, 201-206.